The Disassembly of a Core-Satellite Nanoassembled Substrate for Colorimetric Biomolecular Detection

John R. Waldeisen[1,2,†], *Tim Wang*[2,†], *Benjamin M. Ross*[2], and *Luke P. Lee*[1,2,*]

[1]UC Berkeley/UCSF Graduate Program in Bioengineering

[2]Department of Bioengineering, Biomolecular Nanotechnology Center, Berkeley Sensor and Actuator Center, University of California, Berkeley, California 94720, United States

[†]Authors contributed equally

waldeisen@berkeley.edu, lplee@berkeley.edu

Supporting Information

Scattering Properties of AuNPs: Table S1 depicts the peak position and the FWHM for the four core AuNPs sizes investigated. Core sizes of 30 nm and 50 nm scattered green, whereas the sizes 80 nm and 100 nm appeared chartreuse and minimal redshift was observed upon satellite attachment. 50 nm core particles are optimal for the substrate as they have a larger scattering radius than the 30 nm core particles, which appeared very dim. The calculated scattering cross sections (σ_s) and scattering efficiencies (Q_s) in Table S1 were determined using Mie theory.[31] The scattering efficiency is a proportionality parameter that relates the effective scattering cross section to the actual geometric cross section $\sigma_s = \pi r^2 Q_s$. The optical properties of gold were taken from literature.[32-34]

Table S1. Scattering Properties of Various Sized Core AuNPs

Core AuNP Size [nm]	Peak Position [nm] [a]	FWHM [nm] [a]	Scattering Cross Section, σ_s [nm^2] [b]	Scattering Efficiency, Q_s [b]
30	561.0	97.5	0.94	0.0013
50	556.0	84.6	18.31	0.0093
80	568.3	115.3	249.90	0.0497
100	569.3	110.1	806.05	0.1026

[a] Experimental measurements [b] Calculated using Mie theory

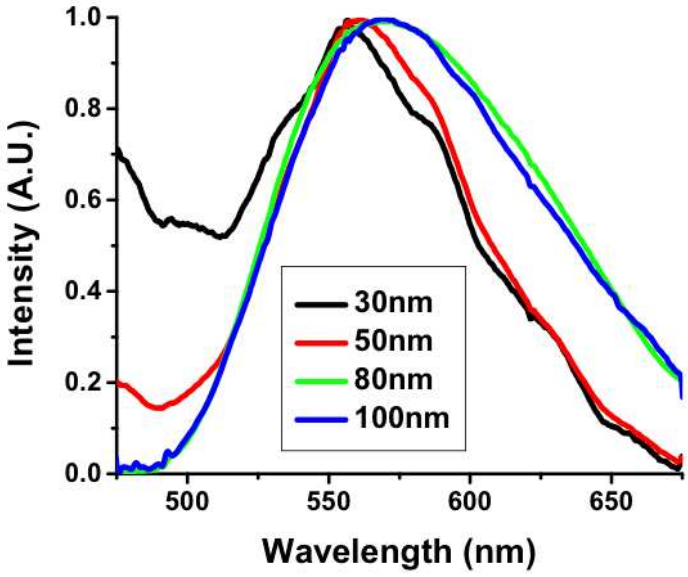

Figure S1. Average of n=10 scattering spectra taken for each of the core AuNPs before satellite attachment. Spectra used to determine peak position and FWHM in Table S1.

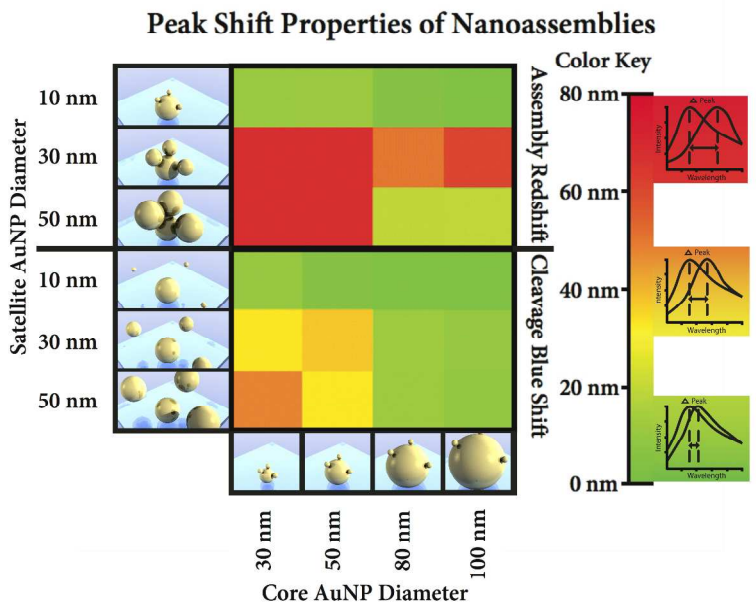

Figure S2. Large-scale characterization study of the DF peak shift properties for a combination of core and satellite diameters. Assembly redshift (top) and disassembly blue shift (bottom) are depicted.

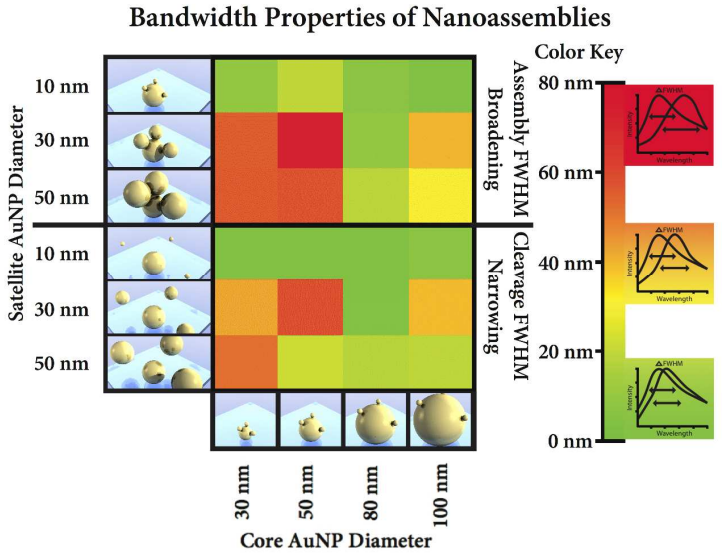

Figure S3. Large-scale characterization study of the FWHM properties for a combination of core and satellite diameters. Assembly FWHM broadening (top) and disassembly FWHM narrowing (bottom) are depicted.

Additional Experimental Data: The sample standard deviations for peak and FWHM measurements are presented in Tables S2 and S3. The calculated deviation is comparatively small given that both had fluctuations as large as 80 nm. Two slides were fabricated for each geometrical variation and random, quintuplicate measurements were acquired per slide.

Table S2. Sample Standard Deviation of Peak Measurements

Satellite AuNP Diameter	30 nm	50 nm	80 nm	100 nm	
10 nm	1.7	0.8	3.5	3.4	Core Deposition [nm]
30 nm	0.7	1.5	2.6	1.0	
50 nm	1.8	1.8	7.4	1.5	
10 nm	5.0	4.3	4.0	4.2	Satellite Attachment [nm]
30 nm	2.4	5.7	3.8	5.0	
50 nm	3.4	4.1	6.9	12.7	
10 nm	2.8	2.9	6.6	1.5	Satellite Release [nm]
30 nm	4.2	5.3	2.4	3.6	
50 nm	2.9	4.0	3.8	2.1	

Core AuNP Diameter

Table S3. Sample Standard Deviation of FWHM Measurements

Satellite AuNP Diameter	30 nm	50 nm	80 nm	100 nm	
10 nm	13.6	12.6	5.4	3.3	Core Deposition [nm]
30 nm	6.2	11.7	5.0	2.6	
50 nm	13.4	3.5	10.5	3.4	
10 nm	24.1	15.5	4.7	2.7	Satellite Attachment [nm]
30 nm	10.6	8.0	7.0	15.9	
50 nm	14.2	7.7	8.3	11.1	
10 nm	18.4	14.3	6.0	4.0	Satellite Release [nm]
30 nm	3.4	6.4	3.2	5.5	
50 nm	4.7	12.2	4.3	4.1	

Core AuNP Diameter

Figure S4 depicts an exemplary PDMS microfluidic device bonded onto the nanoassembled core-satellite substrate. Traditional soft-lithography techniques where employed to create the microfluidic device with channels 150 μm wide and 50 μm high. The PDMS device was oxygen plasma treated and

irreversibly bonded to the substrate. The empty microchannels and the assembled core-satellite AuNP substrate appear as the wider, vertical yellow lines.

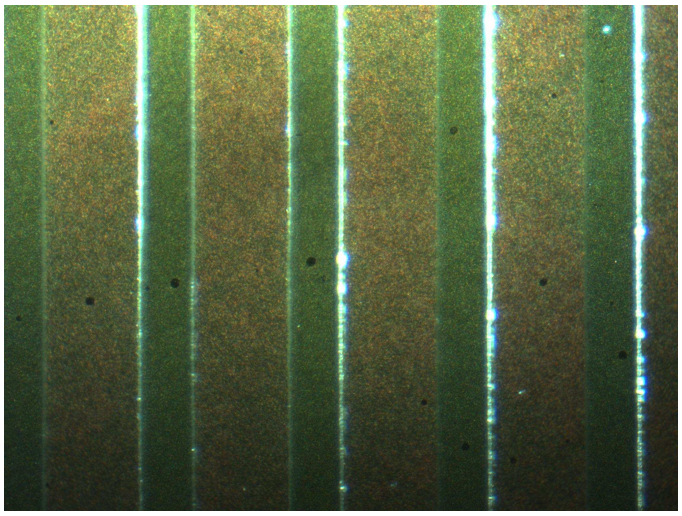

Figure S4. An exemplary PDMS microfluidic device bonded onto the AuNP core-satellite substrate.

The emitted spectrum from the Xenon light source used in the study is shown in Figure S5.

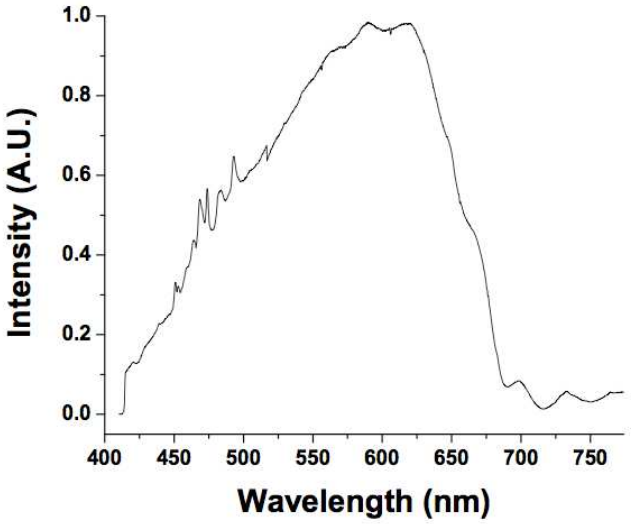

Figure S5. The emission spectra from the Xenon light source used in the study.

The characterization of AuNP fabrication is presented in Table S4 as obtained from the supplier, British Biocell International.

Table S4. Fabrication Data for AuNPs

Core AuNP Size [nm]	Mean Diameter [nm]	Concentration [particles mL^{-1}]	Coefficient of Variation [%]

30	31.1	2E11	< 8
50	49.3	4.5E10	< 8
80	78.8	1.1E10	< 8
100	100.4	5.6E9	< 8

A theoretical analysis of the detection times for a number of prominent proteases found in various bodily fluids is given in Table S5. Using known enzyme kinetics, predicted detection times to cleave a core-satellite substrate specific for each protease were calculated with the equation

$$\frac{V_A}{V_B} = \frac{\left(\frac{K_{cat}}{K_m}\right)_A [E_A][S_A]}{\left(\frac{K_{cat}}{K_m}\right)_B [E_B][S_B]} = \frac{\left(\frac{K_{cat}}{K_m}\right)_A [E_A]}{\left(\frac{K_{cat}}{K_m}\right)_B [E_B]}$$

where V is the velocity of the reaction, k_{cat} is the catalytic constant, k_m is the Michaelis constant, [E] is the enzyme concentration, and [S] is the substrate concentration. The ratio is only valid when the substrate concentration is much less than the Michaelis constant, $[S] << K_m$. Table S5 was determined using the empirically determined time necessary for trypsin to disassemble the core-satellite substrate and resultantly, certain biomolecules were found to be better suited for detection than others. Proteases with higher K_{cat}/K_m values and at greater concentrations in the sample fluid facilitate detection in much less time than other proteases, making them better candidate biomolecules for our proposed detection system.

Table S5. Predicted Detection Times for Physiologically Relevant Biosamples

Enzyme	Bodily Fluid	K_{cat}/K_m [$M^{-1}s^{-1}$]	K_{cat} [s^{-1}]	K_m [M]	Physiological Concentration [μM]	Predicted Detection Time [min]
Trypsin	Digestive	2.1E5	39.9	1.9E-4	104*	50**
Thrombin	Blood	1.3E7	91.0	7.0E-6	2.7	~30
Factor Xa/Va	Blood	1.1E9	81.7	7.6E-8	0.03 - 0.18	>5
Factor IXa/VIIIa	Blood	3.2E7	2.5	8.0E-8	0.0012 - 0.09	>378
MMP-2	Saliva	5.4E4	0.017	1.7E-5	0.00025 - 0.0004	>5.3E8
Acrosin	Semen	1.8E6	77	4.4E-5	1.2	>505

*Concentration used for substrate characterization (not physiological). **Actual time. References: [35-42]

MATLAB scripts were written to normalize and analyze the collected spectral data. Particle density analysis was achieved by employing a particle counting MATLAB script to analyze SEM images taken of the AuNP cores. The scripts are included below.

Supplementary References:

(31) Wang, L. V.; Wu, H. I. *Biomedical Optics: Principles and Imaging;* Wiley & Sons: Hoboken, New Jersey, 2007; pp 17-35.

(32) Schulz, L. G. The Optical Constants of Silver, Gold, and Aluminum. The Absorption Coefficient K. *J. Opt. Soc. Am.* **1954**, *44*, 357-362.

(33) Ordal, M. A.; Long, L. L.; Bell, R. J.; Bell, S. E.; Bell, R. R.; Alexander, R. W., Jr.; Ward, C. A. Optical Properties of the Metals Al, Co, Cu, Au, Fe, Pb, Ni, Pd, Pt, Ag, Ti, and W in the Infrared and Far Infrared. *Appl. Opt.* **1983**, *22*, 1099-1120.

(34) Lynch, D. W.; Hunter, W. R.; *Handbook of Optical Constants of Solids, Vol. 1: Metals;* Palik, E. D., Ed.; Academic Press: San Diego, California, 1998; pp 286-295.

(35) Dang, Q. D.; Vindigni, A.; Di Cera, E. An Allosteric Switch Controls the Procoagulant and Anticoagulant Activities of Thrombin. *Proc. Natl. Acad. Sci. USA* **1995,** *92*, 5977-5981.

(36) Kerschbaumer, R. J.; Riedrich, K.; Kral, M.; Varadi, K.; Dorner, F.; Rosing, J.; Scheiflinger, F. An Antibody Specific for Coagulation of Factor IX Enhances the Activity of the Intrinsic Factor X-activating Complex. *J. Biol. Chem.* **2004,** *279*, 40445-40450.

(37) Nishimura, H.; Takeya, H.; Miyata, T.; Suehiro, K.; Okamura, T.; Niho, Y.; Iwanaga, S. Factor IX Fukuoka: Substitution of ASN^{92} in the Second Epidermal Growth Factor-like Domain Results in Defective Interaction with Factors VIIIa/X. *J. Biol. Chem.* **1993,** *268*, 24041-24046.

(38) Butenas, S.; Ribarik, N.; Mann, K. G. Synthetic Substrates for Human Factor VIIa and Factor VIIa-Tissue Factor. *Biochemistry* **1993,** *32*, 6531-6538.

(39) Nagase, H.; Fields, C. G.; Fields, G. B. Design and Characterization of a Fluorogenic Substrate Selectively Hydrolyzed by Stromelysin 1 (Matrix Metalloproteinase-3). *J. Biol. Chem.* **1994,** *269*, 20952-20957.

(40) Rai, B.; Kharb, S.; Jain, R.; Anand, S. C. Biomarkers of Periodontitis in Oral Fluids. *J. Oral Sci.* **2008,** *50*, 53-56.

(41) Liu, D. Y.; Baker, H. W. G. Relationships Between Human Sperm Acrosin, Acrosomes, Morphology, and Fertilization in vitro. *Hum. Reprod.* **1990,** *5*, 298-303.

(42) Hardy, D. M.; Schoots, A. F. M.; Hedrick, J. L. Caprine Acrosin: Purificaiton, Characterization and Proteolysis of the Porcine Zona Pellucida. *Biochem. J.* **1989,** *257*, 447-453.

----------MATLAB Code for the Determination of Peak Location and FWHM----------

```
%Clear all previous screens
close all
clear all
clc

[filenameLS, pathnameLS] = uigetfile('*.txt','Select Background Lightsource','/Users/ Desktop/');
infoLS = dlmread([pathnameLS filenameLS]);
[rowsizeLS colsizeLS] = size(infoLS);

[filenameFF, pathnameFF] = uigetfile('*.txt','Select Flatfield','/Users/Desktop/');
infoFF = dlmread([pathnameFF filenameFF]);
[rowsizeFF colsizeFF] = size(infoFF);

%Open ASCII-delimited spectra data
[filename, pathname, filterindex] = uigetfile({'*.txt'},'Select Spectra to
Analyze','/Users/Desktop/','MultiSelect','on');
numfiles = max(size(filename));

result = ones([numfiles 3]);

for iter = 1:1:numfiles

   filename(iter)
   info = dlmread([pathname char(filename(iter))]);
   [rowsize colsize] = size(info);
   normdata = (info(1:rowsize,colsize)-infoFF(1:rowsizeFF,colsizeFF))./(infoLS(1:rowsize,colsize)-
infoFF(1:rowsizeFF,colsizeFF));

   fig = figure;
   hold on;
   smoothdata = smooth(normdata(1:rowsize));
   smoothplot = plot(info(1:rowsize,1), smoothdata(1:rowsize),'Color', 'r','LineWidth',2);
   rawdata = plot(info(1:rowsize,1), normdata(1:rowsize));

   %[maxyaxis,maxI] = max(smoothdata(300:900));
   [maxyaxis,maxI] = max(smoothdata(300:900));

   maxI = maxI + 299;
%    [minyaxis,minI] = min(smoothdata(147:977));
   [minyaxis,minI] = min(smoothdata(54:977));
   minI = minI + 146;
   ylim([minyaxis maxyaxis]);
   xlim([info(1,1) info(rowsize,1)]);

   halfmax = ((maxyaxis - minyaxis)./2) + minyaxis;
   refline(0,halfmax);

%    [localmin, locminI] = min(smoothdata(237:400));
   [localmin, locminI] = min(smoothdata(30:400));
```

```
%    locminI = locminI + 236;
   locminI = locminI + 29;

   xlabel('Wavelength (nm)');
   ylabel('Semi-Normalized Intenisty');

   %Search for intersects with halfmax
   for itera = locminI:1:977
      if (smoothdata(itera) < halfmax && smoothdata(itera + 1) > halfmax) | (smoothdata(itera) >
halfmax && smoothdata(itera + 1) < halfmax)
         itera;
         wavelength = info(itera,1)
         intensity = smoothdata(itera);

         ref(1:rowsize,1) = wavelength;
         for iteration = 1:1:rowsize
            ref(iteration,2) = iteration./rowsize;
         end

         refplot = plot(ref(1:rowsize,1), ref(1:rowsize,2),'Color','g','Linewidth',2);

        %Fill in results matrix; elseif prevents excess right intersect points written to matrix
         if result(iter,1) == 1;
            result(iter,1) = wavelength;
         elseif result(iter,2) < 500
            result(iter,2) = wavelength;
         end
      end
   end

   %If leftside spectrum does not intersect halfmax, applies linear extrapolation
   if result(iter,1) > 600;
      i1 = 255
      i2 = 310
%       i1 = 439;
%       i2 = 476;
      result(iter,2) = result(iter,1);
      slopedif = smoothdata(i2) - smoothdata(i1);
      slopeleft = slopedif./(info(i2) - info(i1));
      distleft = (smoothdata(i2) - halfmax)./slopeleft;
      actwavelengthleft = info(i2) - distleft;
      result(iter,1) = actwavelengthleft;
      actrefleft(1:rowsize,1) = actwavelengthleft;

      for actiteration = 1:1:rowsize;
         actrefleft(actiteration,2) = actiteration./rowsize;
      end

      actrefplotleft = plot(actrefleft(1:rowsize,1), actrefleft(1:rowsize,2),'Color','g','Linewidth',2);
      plot([actwavelengthleft info(i2)],[halfmax smoothdata(i2)],'Color','y','Linewidth',2);
   end
```

```
%If rightside spectrum does not intersect halfmax before LS fluctuations, applies linear extrapolation
   if result(iter,2) > info(970) | result(iter,2) ==1;
      slopediff = smoothdata(958) - smoothdata(939);
      slope = slopediff./(info(958)-info(939));
      dist = (smoothdata(958) - halfmax)./-slope;
      actwavelength = dist + info(958);
      result(iter,2) = actwavelength;
      actref(1:rowsize,1) = actwavelength;

      for actiteration = 1:1:rowsize;
         actref(actiteration,2) = actiteration./rowsize;
      end

      actrefplot = plot(actref(1:rowsize,1), actref(1:rowsize,2),'Color','g','Linewidth',2);
      plot([info(958) actwavelength],[smoothdata(958) halfmax],'Color','y','Linewidth',2);
      xlim([info(1,1) (actwavelength + 10)]);
   end

   result(iter,3) = result(iter,2)-result(iter,1);
end

%Result is matrix of left, right intercepts, and FWHM
result
FWHM = sum(result(1:5,3))./5
SD = std(result(:,3),1)
%SD1 = sqrt(sum((result(:,3) - FWHM).^2)./numfiles)
```

```
----------MATLAB Script for Determining Core Density from SEM Images----------
clear all
close all
clc

[filename, pathname] = uigetfile('*.tif','Select SEM Image','/Users/Waldie/Desktop/MMP GNP
Detection Data/SEM/');
I = imread([pathname filename]);

figure
imshow(I)

figure
BW = im2bw(I);
imshow(BW)

hold on
[L,num] = bwlabel(BW)
area = regionprops(L,'Area')

count = 0

for iter = 1:num
   if area(iter).Area > 25
      count = count +1
   end
end


for row = 1:512
   for col = 1:512
      if L(row, col) > 0 & area(L(row,col)).Area > 25
         plot(col, row)
      end
   end
end
```